



Dynamics of interacting scalar field model in the realm of chiral cosmology

Trupti Patil^{1,a}, Sukanta Panda^{1,b}, Manabendra Sharma^{2,3,c}, Ruchika^{4,d}

¹ Department of Physics, IISER Bhopal, Bhopal 462066, India

² Inter University Centre for Astronomy and Astrophysics, Post Bag 4, Pune 411007, India

³ NAS, Centre for Theoretical Physics and Natural Philosophy, Mahidol University, Nakhonsawan Campus, Nakhonsawan 60130, Thailand

⁴ Department of Physics, Indian Institute of Technology, Bombay, Mumbai 400076, India

Received: 14 September 2022 / Accepted: 24 January 2023 / Published online: 10 February 2023
© The Author(s) 2023

Abstract The strange behaviour of the universe's dark sector offers us the flexibility to address cosmological problems with different approaches. Using this flexibility, we consider a possible exchange of energy among the dark sector components as a viable candidate model. In the present work, we investigate the interaction between two scalar fields within the generalization of a two-component chiral cosmology. We also show that there exists a unique equivalence between fields and fluids description of interacting dark sector model. Later, a detailed analysis of the dynamics of the dark energy-dark matter model with coupling in both kinetic and potential parts has been performed using a method of qualitative analysis of dynamical systems. Moreover, the cosmological viability of this model is analyzed for the potential of an exponential form via the phase-space study of autonomous system for various cosmological parameters.

1 Introduction

After the discovery of the accelerated expansion of the universe at the very end of the twentieth century, various theoretical models have been recommended to comply with the experimentally obtained evidences [1–11] and to set up a new context for the physics of the future. In the quest to explain recent cosmological observations, a novel concept of dark energy with negative pressure has been introduced and studied closely in the literature [12, 13]. The mysterious nature of this dark entity has multiplied the area of research with a

focus on uncovering its properties and it has been one of the hot topics in modern cosmology. Among the various choices for dark energy (DE), the cosmological constant is the one that favours the observations most [14]. Nevertheless, as seen from the theoretical point of view, it consists of two fundamental problems in cosmology, (1) cosmological constant problem [15, 16] and (2) coincidence problem [17–21].

To overcome these problems various other canonical [22, 23] and non-canonical scalar field models [24, 25] were introduced. It has been suggested and studied that dark energy could be dynamic and evolve with time. This feature has been studied in model where equation of state parameter ω_ϕ ranges as $-1 < \omega_\phi < -\frac{1}{3}$ [22, 23, 26, 27] and leads to beat the cosmological constant problem. The various other dark energy scalar field model viz. k-essence, phantom, quintom, tachyon, galileon, and multi-scalar field models [28–37], where the non-canonical kinetic term appears as a coupling factor have also been studied meticulously and found to be very useful to ease the coincidence problem. However, there are recent studies that argue a large class of Dark Energy Models, including Quintessence and K-essence [38–41]. More often than not we address those models as dark energy–dark matter interaction models. Various DE interacting scalar field models [22, 25, 42–45] and phenomenological fluid models [46–52] have been set forth and studied in literature. Another approach to address this issue is based on modified gravity (see Refs. [53–55] and references therein).

The dynamics of chiral cosmology has been studied earlier in [56–59]. It has been noticed that chiral cosmology can provide a suitable realm for the description of the multi-scalar field model and draw the framework where characteristics of the dark sector universe can be explained under the generalization of the chiral cosmological model.

^a e-mail: trupti19@iiserb.ac.in (corresponding author)

^b e-mail: sukanta@iiserb.ac.in

^c e-mail: sharma.manabendra1501@yahoo.com

^d e-mail: ruchika@ctp-jamia.res.in

In our work, we are interested in the background dynamics of field equations in general relativity in a spatial flat Friedmann–Lemaître–Robertson–Walker (FLRW) (homogeneous and isotropic) universe. Motivated by quintom paradigm [60], in our analysis, we aim to study a two-field interaction model under the chiral cosmological framework. We consider a case where the coupling factor lives in kinetic as well in potential parts of the fields. The findings, e.g. in [61] and the study of [62] show that such DDI models are indeed more capable than was known up till that can solve current recurring problems in cosmology, e.g. coincidence problem and thus, in our opinion, makes it an interesting study to probe further.

The equivalence between the phenomenological fluid model and the 2-field scalar field model provides us with the interaction term which is a mixture of the dark energy field and dark matter fluid energy density [63]. In such a scenario, the rigorous form of the Einstein field equations is turned into an autonomous system of equations by defining preferable dimensionless variables. In particular, we have found that the simple dynamical system evaluation [13,64] of an interacting DE–DM model issues the physical validity of the discussed cosmological DE model in late-time cosmology. The theory can be applicable to address the current cosmological problems as long as the background dynamics are studied, where we notice sufficiently long, extended era of matter dominated universe to the current era of an accelerated expanding universe. Additionally, we have examined that the big rip singularity problem does not appear in our model. The plan of the work is structured as follows: In Sect. 2, we describe the chiral cosmology and set up dynamical equations for the two-field chiral model. In Sect. 3, we consider a coupled dark energy (DE)–dark matter (DM) model and obtain evolution equations. Section 4 systematically shows a one-to-one correspondence between the fluid and field theory approaches. The principal analysis of our work is presented in Sect. 5. It explains the formulation of an autonomous system consisting of non-linear coupled differential equations. The examination of critical points of the system and their stability analysis have also been shown in this section. In the subsection, we show the graphical representation of the obtained results to complement the physical viability of the model. The final Sect. 6, summarizes the present work and outlines the conclusion.

2 Chiral cosmology

The gravitational action integral for the chiral cosmological model reads as:

$$S = \int d^4x \sqrt{-g} \left(\frac{R}{2} - \frac{1}{2} g^{\mu\nu} F_{AB}(\varphi) \nabla_\mu \varphi^A \nabla_\nu \varphi^B - V(\varphi) \right), \tag{2.1}$$

where, R is the Ricci scalar. $g_{\mu\nu}$ is the metric tensor of the 4-D space-time along with $F_{ab}(\varphi)$ being the second-rank tensor of chiral space where the scalar field evolve. $V(\varphi)$ is the potential. Here, we use the natural units where $c = 1$ and the reduced Planck mass $M_p^2 = \frac{1}{8\pi G} = 1$.

The individual variation of Eq. (2.1) w.r.t. the metric tensor and the scalar fields φ^A brings us the Einstein’s gravitational field equations and the Klein–Gordon equation as:

$$G_{\mu\nu} = T_{\mu\nu} \equiv F_{AB}(\varphi) \nabla_\mu \varphi^A \nabla_\nu \varphi^B - g_{\mu\nu} \left(\frac{1}{2} g^{\mu\nu} F_{AB}(\varphi) \nabla_\mu \varphi^A \nabla_\nu \varphi^B + V(\varphi) \right), \tag{2.2}$$

$$g^{\mu\nu} \left(\nabla_\mu F_B^A(\varphi) \nabla_\nu \varphi^B \right) - F_B^A(\varphi) \frac{\partial V(\varphi)}{\partial \varphi^B} = 0. \tag{2.3}$$

The line element for the chiral space is given as:

$$ds_c^2 = F_{AB}(\varphi) d\varphi^A d\varphi^B, \quad A, B = 1, 2, \dots, N. \tag{2.4}$$

2.1 2-Field chiral model

To study the interaction between the dark sector fields, we consider a two scalar field chiral cosmological model. A possible interaction in both kinetic and potential parts can be seen between the two fields [63,65] which can be an effective mechanism to explain the coincidence problem and cosmological constant problem. For further analysis of the model we set,

$$\varphi^1 = \phi \quad \text{and} \quad \varphi^2 = \psi \quad \text{and} \\ F_{11} = A(\phi, \psi), \quad F_{22} = B(\phi, \psi), \quad F_{12} = C(\phi, \psi) = F_{21}.$$

Following the analysis in the chiral space, for an isotropic and homogeneous universe, the space-time (2.4) gives us the spatially flat FLRW space-time with the line element as

$$ds^2 = -dt^2 + a^2(t)(dx^2 + dy^2 + dz^2). \tag{2.5}$$

where $a(t)$ defines the scale factor as a function of cosmic time.

The gravitational action integral (2.1) in the case of two scalar fields then becomes:

$$S = \int d^4x \sqrt{-g} \left(\frac{R}{2} - \frac{1}{2} g^{\mu\nu} A(\phi, \psi) \phi_{,\mu} \phi_{,\nu} - \frac{1}{2} g^{\mu\nu} B(\phi, \psi) \psi_{,\mu} \psi_{,\nu} - g^{\mu\nu} C(\phi, \psi) \phi_{,\mu} \psi_{,\nu} - V(\phi, \psi) \right). \tag{2.6}$$

Also, Eq. (2.2) provides us the Einstein’s gravitational field equation as:

$$G_{\mu\nu} = T_{\mu\nu} \equiv A\phi_{,\mu}\phi_{,\nu} + B\psi_{,\mu}\psi_{,\nu} + 2C\phi_{,\mu}\psi_{,\nu} - g_{\mu\nu}\left(\frac{1}{2}g^{\mu\nu}(A\phi_{,\mu}\phi_{,\nu} + B\psi_{,\mu}\psi_{,\nu} + 2C\phi_{,\mu}\psi_{,\nu}) + V(\phi, \psi)\right). \tag{2.7}$$

Furthermore, Eq. (2.3) provides the Klein–Gordon equations in the FRW universe as:

$$3H(A\dot{\phi} + C\dot{\psi}) + \partial_t(A\dot{\phi} + C\dot{\psi}) - \frac{1}{2}\frac{\partial A}{\partial\phi}\dot{\phi}^2 - \frac{\partial C}{\partial\phi}\dot{\phi}\dot{\psi} - \frac{1}{2}\frac{\partial B}{\partial\phi}\dot{\psi}^2 + \frac{\partial V}{\partial\phi} = 0, \tag{2.8}$$

$$3H(C\dot{\phi} + B\dot{\psi}) + \partial_t(C\dot{\phi} + B\dot{\psi}) - \frac{1}{2}\frac{\partial A}{\partial\psi}\dot{\phi}^2 - \frac{\partial C}{\partial\psi}\dot{\phi}\dot{\psi} - \frac{1}{2}\frac{\partial B}{\partial\psi}\dot{\psi}^2 + \frac{\partial V}{\partial\psi} = 0, \tag{2.9}$$

where, $H = \frac{\dot{a}}{a}$ is the Hubble rate.

In the next section, we consider a two scalar fields interacting model where both the fields are coupled to each other. The coupling can be observed either in kinetic or in potential or in both parts of the setup Lagrangian. This kind of model has been considered before as well in literature [33, 58, 66]. The objective behind studying such a model is to achieve the negative running of the equation of state (EoS) parameter which is also consistent with present observational scenarios.

3 Construction of DE–DM interaction model

As inspired by chiral cosmology [56–59], we work with a model where the parameters in Eq. (2.6) take value as:

$$A = -1, \quad B = B(\phi), \quad C = 0,$$

for which action integral is given as:

$$S = \int d^4x \sqrt{-g} \left(\frac{R}{2} + \frac{1}{2}g^{\mu\nu}\phi_{,\mu}\phi_{,\nu} - \frac{1}{2}B(\phi)g^{\mu\nu}\psi_{,\mu}\psi_{,\nu} - V(\phi) - \alpha\phi^2\psi^2 \right). \tag{3.1}$$

One of our prime goals is to work on assimilating DE–DM interaction in action (3.1). In order to accomplish our goal to design a DE–DM interaction (DDI) model, we here, consider one of the fields as a dark energy candidate and another one as a dark matter candidate. The details about the roles played by the fields have been discussed in the following section. The last term in Eq. (3.1) represents an interacting potential.

Now, from the line element (2.5) and modified action (3.1), the dynamical field equations for the fields ϕ and ψ are given, respectively, as in Eqs. (3.2) and (3.3)

$$\nabla_\mu \nabla^\mu \phi + \frac{B_{,\phi}}{2} \nabla_\mu \psi \nabla^\mu \psi + 2\alpha\phi\psi^2 + V_{,\phi} = 0, \tag{3.2}$$

$$\nabla_\mu \nabla^\mu \psi + \frac{B_{,\phi}}{B} \nabla_\mu \psi \nabla^\mu \phi - 2\alpha\psi\phi^2 B^{-1} = 0, \tag{3.3}$$

where, ‘ $\cdot_{,\phi}$ ’ denotes the partial derivative w.r.t ϕ . Whereas the Friedmann equations are given as in Eqs. (3.4) and (3.5)

$$3H^2 = \frac{-\dot{\phi}^2}{2} + \frac{B(\phi)}{2}\dot{\psi}^2 + V(\phi) + \alpha\phi^2\psi^2, \tag{3.4}$$

$$2\dot{H} + 3H^2 = -\left(\frac{-\dot{\phi}^2}{2} + \frac{B(\phi)}{2}\dot{\psi}^2 - V(\phi) - \alpha\phi^2\psi^2\right). \tag{3.5}$$

The field-theoretic description of dark energy coupled to dark matter treats both components as scalar fields. As the interaction is proposed between these fields, it is observed that the dark energy (DE) and dark matter (DM) do not satisfy the energy–momentum tensor conservation equation independently, instead, they satisfy the local conservation equation in the form given as:

$$-\nabla^\mu T_{\mu\nu}^{(\phi)} = Q_\nu = \nabla^\mu T_{\mu\nu}^{(\psi)}, \tag{3.6}$$

where,

$$Q_\nu = \nabla^\mu T_{\mu\nu}^{(\psi)} = -\left(\frac{B_{,\phi}}{2}\nabla_\xi\psi\nabla^\xi\psi + 2\alpha\phi\psi^2\right)\nabla_\nu\phi, \tag{3.7}$$

stands in for the energy transfer between dark energy and dark matter in interacting dark zone. Here, $T_{\mu\nu}^{(\psi)}$ and $T_{\mu\nu}^{(\phi)}$ play the role of energy–momentum tensor of field ψ and field ϕ , respectively.

Now, evolved from Eq. (3.7), we can write the conservation equations for the fields ϕ and ψ in FLRW space-time, respectively, as:

$$-\ddot{\phi} - 3H\dot{\phi} - \frac{B_{,\phi}}{2}\dot{\psi}^2 + 2\alpha\phi\psi^2 + V_{,\phi} = 0, \tag{3.8}$$

$$\ddot{\psi} + 3H\dot{\psi} + \frac{B_{,\phi}}{B}\dot{\phi}\dot{\psi} + 2\alpha\psi\phi^2 B^{-2} = 0. \tag{3.9}$$

4 Similitude between field theory strategy and phenomenological fluid strategy

This section outlines one-to-one scaling between the field theory approach and the fluid approach of the interacting dark sector. This type of work has also been modeled and studied before in [63]. We, here, try to illustrate that the interaction function Q_ν , achieved with the assistance of classical field theory exhibits a unique form when the fluid approach has been applied to the interacting dark sector model under consideration. Also, the above-mentioned interaction function

Q_v has been derived systematically from the series of equations starting from action integral to conservation equations where one of the fields becomes dark matter representative.

Now, starting up with the fluid description of the above interacting DE–DM model, one of the fields can be described as phenomenological fluid. In such description, it is often suitable to consider the dark matter as a fluid component. The openness in the work provides the freedom where we can assume either the field “ ϕ ” or the field “ ψ ” as a dark matter entity. Therefore, we substitute the dark matter fluid for the scalar field “ ψ ”. Thus, framing the field “ ϕ ” as a DE entity. In this description, the dark matter energy density ρ_{dm} and pressure P_{dm} are given as follows:

$$\rho_{dm} = -\frac{1}{2}B(\phi)\left(g^{\mu\nu}\nabla_\mu\psi\nabla_\nu\psi - 2\alpha\phi^2\psi^2B^{-1}\right), \quad (4.1)$$

$$P_{dm} = -\frac{1}{2}B(\phi)\left(g^{\mu\nu}\nabla_\mu\psi\nabla_\nu\psi + 2\alpha\phi^2\psi^2B^{-1}\right), \quad (4.2)$$

whereas the energy–momentum tensor (2.7) for the DDI model in terms of DE scalar field (ϕ) and DM fluid can be revised as:

$$T_{\mu\nu} = \left(-\nabla_\mu\phi\nabla_\nu\phi + \frac{1}{2}g_{\mu\nu}\nabla_\xi\phi\nabla^\xi\phi - g_{\mu\nu}V(\phi) + P_{dm}g_{\mu\nu} + (\rho_{dm} + P_{dm})u_\mu u_\nu \right), \quad (4.3)$$

where u_μ is termed as the four-velocity of the DM fluid.

As observed in the literature, the phenomenological fluid models state the interaction term “ Q_v ” as a linear function of DM density or DE density or both. Also, it has been seen that the “ Q_v ” in fluid models is not uniquely acquired considering that it is simply set by hand. Unlike in fluid models, the interaction term “ Q_v ” derived in (4.4) has a particular form that is acquired by correlating the fields and fluids for the present interacting model.

This analogy between fields and fluids assists us to revised all the dynamical field equations and conservation equations in terms of dark matter fluid component and dark energy field component for the DDI model. Here, in our work, we consider dark matter as a pressure-less entity.

Now, from Eq. (3.7), interaction function Q_v can be revised as:

$$Q_v = \left(\frac{B,\phi}{B} - \frac{2}{\phi} \right) \frac{\rho_{dm}}{2} \nabla_\nu\phi, \quad (4.4)$$

and the Friedmann equations and the conservation equations in the FLRW space-time then revised, respectively, as in (4.5) and (4.6)

$$3H^2 = \rho_{dm} - \frac{\dot{\phi}^2}{2} + V(\phi),$$

$$3H^2 + 2\dot{H} = -\left(P_{dm} - \frac{\dot{\phi}^2}{2} - V(\phi) \right). \quad (4.5)$$

$$-\ddot{\phi}\phi - 3H\dot{\phi}^2 + V,\phi\dot{\phi} = Q,$$

$$\dot{\rho}_{dm} + 3H\rho_{dm} = -Q. \quad (4.6)$$

Here, it is noted that the DE component “ ϕ ” has negative kinetic term, thus it is phantom field. Though the phantom field “ ϕ ” exhibits instabilities in quantum field arena [67,68], could be stable in classical field theory and may clearly be represented by a scalar field with negative kinetic energy term (Eq. 4.5). In such models, the evolution of the universe is phantom dominated with $\omega_\phi < -1$ [69]. It is interesting to know that the cosmological evolution of ω_ϕ (w.r.t. red-shift(z)) less than -1 is very much acknowledged by the observations [70–75]. Though this feature can exhibit an unusual dynamics as it violates the energy conditions [67,76–78], the exotic form of dark energy in terms of phantom fields are profoundly studied in the literature seeing the approval from latest observational findings [74,75,77] and leads to the required current accelerated expansion of the universe. (Nevertheless, it has been investigated [67,79] that it is not harmless for an energy component to violate the dominant energy condition (DEC) or weak energy condition (WEC) that too for a finite time period.) So, here, the motivation to consider such an exotic form of energy is strongly driven by the observations.

It can also be realized from the EoS parameter less than -1 that the phantom energy density may rise to diverge with time, possibly causing big rip singularity in finite time in future [80,81]. However, it has been shown by various studies that this can be over-passed, for details see [82,83]. However, in this work, we have shown that the problem of big rip singularity does not occur.

5 Dynamical system formulation

The cosmological equations pertaining to the evolution of an isotropic and homogeneous universe are purely a network of ordinary differential equations. An impressive technique to study such networks is by moulding them into an autonomous (dynamical) system. The mathematical background behind the dynamical systems helps us to realize the qualitative features of the cosmological model under analysis. To study the dynamics of the system, we present the following set of expansion normalized variables

$$x = \frac{\dot{\phi}}{\sqrt{6}H}, \quad y = \frac{\sqrt{V(\phi)}}{\sqrt{3}H}, \quad \Omega_m = \frac{\rho_{dm}}{3H^2}, \quad (5.1)$$

where, using Eqs. (4.5) and (4.6) the equivalent form of the field equations for an interacting DE–DM model become:

$$x' = -\sqrt{\frac{3}{2}}\left(\lambda y^2 + \frac{I}{x}\right) - \frac{3}{2}x(1 + x^2 + y^2), \quad (5.2)$$

$$y' = -\sqrt{\frac{3}{2}}(\lambda xy) + \frac{3}{2}y(1 - x^2 - y^2), \tag{5.3}$$

$$\Omega'_m = -3\Omega_m(x^2 + y^2) - \sqrt{6}I, \tag{5.4}$$

$$\lambda' = \sqrt{6}\lambda^2x(1 - \Gamma_\lambda), \tag{5.5}$$

$$k' = \sqrt{6}k^2x(1 - \Gamma_k), \tag{5.6}$$

$$\beta' = \sqrt{6}\beta^2x(1 - \Gamma_\beta), \tag{5.7}$$

$$\alpha' = -\sqrt{6}\alpha\beta x, \tag{5.8}$$

in which λ, k, β and α are defined as

$$\begin{aligned} \lambda(\phi) &= -\frac{V_{,\phi}}{V(\phi)}, & k(\lambda) &= -\frac{B_{,\phi}}{B(\phi)}, \\ \beta(\phi) &= -\frac{\alpha_{,\phi}}{\alpha(\phi)}, & \alpha &= \alpha(\phi), \end{aligned} \tag{5.9}$$

and the functions $\Gamma_\lambda, \Gamma_k, \Gamma_\beta$ are defined as

$$\Gamma_\lambda = \frac{V_{,\phi\phi} V}{V_{,\phi}^2}, \quad \Gamma_k = \frac{B_{,\phi\phi} B}{B_{,\phi}^2}, \quad \Gamma_\beta = \frac{\alpha_{,\phi\phi} \alpha}{\alpha_{,\phi}^2}. \tag{5.10}$$

Here, prime denotes derivative with respect to the number of e-foldings $N = \ln(a)$ and ‘ ϕ ’ denotes the partial derivative w.r.t ϕ .

We write the scaled interaction term (I) as

$$I = \frac{(2\beta - k)}{2} \Omega_m x = \frac{1}{3} \frac{Q}{\sqrt{6}H^3}, \tag{5.11}$$

where ‘ Ω_m ’ symbolizes the relative density parameter for the dark matter component. It has been shown in Fig. 5 that Ω_m varies almost steadily at late times. Please note that this feature has been taken into account for the further phase-space analysis of the system in Sect. 5.3.

Also, Eq. (5.1) provides us the Friedmann constraint in terms of density parameter for dark matter as

$$1 + x^2 - y^2 = \Omega_m. \tag{5.12}$$

Now, we compile other cosmological parameters in terms of dynamical variables (5.1).

The density parameter for the phantom field (DE) can be written as:

$$\Omega_\phi = -x^2 + y^2, \tag{5.13}$$

with the equation of state parameter ω_ϕ as:

$$\omega_\phi = \frac{-x^2 - y^2}{-x^2 + y^2}. \tag{5.14}$$

Then the effective equation of state parameter for the DE–DM interaction model becomes:

$$\omega_{eff} = \frac{P_{eff}}{\rho_{eff}} = \frac{P_\phi}{\rho_\phi + \rho_m}, \tag{5.15}$$

$$\omega_{eff} = -x^2 - y^2, \tag{5.16}$$

and the deceleration parameter is:

$$q = -1 + \frac{3}{2}(1 + \omega_{eff}). \tag{5.17}$$

It can be seen that the acceleration condition is feasible for negative ‘ q ’ values i.e., for $q < 0$, whereas the deceleration condition is feasible for positive ‘ q ’ values i.e., for $q > 0$.

5.1 Critical points and stability analysis

Now, we submit the comprehensive phase-space study of the dynamical system (5.2)–(5.8) (for such phase-space analysis, refer [13,64,84]). The 7D autonomous system for an interacting DE–DM model is very much tangled and analysing the stability of the critical points is again a trickier work. In order to facilitate the further analysis, an exponential potential of the form $V(\phi) = V_0 e^{\alpha(\phi)} = V_0 e^{c'\phi}$ is the most suitable choice [13,64]. However, for the current study, ‘ $\alpha(\phi)$ ’ is taken to be a non-zero constant to additionally reduce the dimensionality of the system. By default Eqs. (5.5), (5.7) and (5.8), then becomes trivial fetching us an apt 4D autonomous system.

Though such a model has been considered before in [63], the rigorous fixed-point analysis and stability analysis for this distinct exemplar has not been performed. Such analysis is essential to understand the mystifying dynamics of the observable universe in depth. Following this, we now find out the critical points and discuss their existence and stability properties. The system contains four critical points ‘A’, ‘B’, ‘C’ and ‘D’ in the phase space depending on the values of ‘ λ ’ and ‘ β ’ as presented in the Table 1. In the following, we examine the existence and acceleration features of each of the fixed points corresponding to their eigenvalues in the parameter space (β, λ) as presented in Table 2.

Critical point A exist for all real values of parameter β . The point is completely scarce of scalar field ϕ as there is no contribution either from kinetic energy or from the potential energy of the field. For pressure-less DM, the effective EoS (ω_{eff}) vanishes which implies that the point does not facilitate the condition for accelerating universe. Following the constraint equation (5.12), the relative density parameter for DM becomes one and hence the point can be a representative of the DM-dominated universe in the past. The critical point A is of non-hyperbolic nature. For the condition, $(\beta, \Omega_m) \neq 0$, only one of the eigenvalues is zero (Table 2). Thus, the critical line corresponding to the point A fits with the Ω_m axis and the imposition of the centre manifold theory becomes an impracticable job (for details, refer [64, Sec. 4.4]). This implies that for $\Gamma_k < 1$, the critical line of the point A acts as a saddle line but for $\Gamma_k > 1$, the eigenvalues show complex nature

Table 1 The critical points and cosmological parameters corresponding to an autonomous system of an interacting DE–DM model with an exponential potential and constant α

Critical points	x	y	Ω_m	Ω_ϕ	k	ω_{eff}
A	0	0	Ω_m	0	2β	0
B	$-\sqrt{\frac{2}{3}}\beta$	0	$1 + \frac{2}{3}\beta^2$	$-\frac{2}{3}\beta^2$	0	$-\frac{2}{3}\beta^2$
C	$\frac{-\sqrt{\frac{3}{2}}}{\beta-\lambda}$	$\frac{\sqrt{-\frac{3}{2}+\beta^2-\beta\lambda}}{(\beta-\lambda)}$	$\frac{3-\beta\lambda+\lambda^2}{(\beta-\lambda)^2}$	$\frac{-3+\beta^2-\beta\lambda}{(\beta-\lambda)^2}$	0	$\frac{1}{\frac{\lambda}{\beta}-1}$
D	$\frac{-\lambda}{\sqrt{6}}$	$\sqrt{1 + \frac{\lambda^2}{6}}$	0	1	0	$-1 - \frac{\lambda^2}{3}$

Table 2 The existence and eigenvalues of corresponding critical points

Critical pts.	Existence	Accel.	Eigenvalues
A	$\forall\beta$	No	$\frac{3}{2}, 0, -\frac{3}{4} \pm \frac{\sqrt{3}}{4}\sqrt{3 + 32\beta^2\Omega_m(1 - \Gamma_k)}$
B	$\forall\beta$	Yes	$0, -2\beta^2, -\frac{3}{2} - \beta^2, \frac{3}{2} - \beta^2 + \lambda\beta$
C	$\frac{\lambda}{\beta} > -2$	Yes	See Appendix
D	$\forall\lambda$	Yes	$0, -3 - \frac{\lambda^2}{2}, -3 - \lambda^2 + \beta\lambda, -3 - \lambda^2,$

with the real parts predicting the stability of the point A as saddle one.

Critical point B is dominated by the kinetic energy of the scalar field ϕ . Its existence, like point A, is valid for any real value of parameter β . The point pictures the existence of an accelerating solution ($\omega_{eff} < -\frac{1}{3}$), locating in the region of parameter space where the condition $\beta^2 > \frac{1}{2}$ is being satisfied. This condition can lead us to both, quintessence and phantom dominated DE accelerating universe. The critical point B is also non-hyperbolic in nature like point A and the Centre Manifold Theory can be employed to reveal the nature of point B.

Critical point C is valid for $-2 < \frac{\lambda}{\beta} < 1$ in the phase-space. It exhibits the scaling solution where the ratio between DE and DM density parameter throws a constant

$$\frac{\Omega_\phi}{\Omega_m} = \frac{-3 + \beta^2 - \beta\lambda}{3 + \lambda^2 - \beta\lambda}.$$

The accelerated evolution of the universe for the point C is possible within the above set limit for $\frac{\lambda}{\beta}$.

When $\frac{\lambda}{\beta}$ becomes zero. The DE i.e. scalar field ‘ ϕ ’ portrays the cosmological constant behaviour ($\omega_{eff} = -1$) and an accelerated de Sitter universe is achieved.

For $0 < \frac{\lambda}{\beta} < 1$ case, ω_{eff} ranges as $\omega_{eff} < -1$, clearly showcasing the phantom DE dominated behaviour. Whereas, for $-2 < \frac{\lambda}{\beta} < 0$ case, ω_{eff} ranges as $-1 < \omega_{eff} < -\frac{1}{3}$ and suits the condition under which scalar field (DE) behaves as a quintessence field.

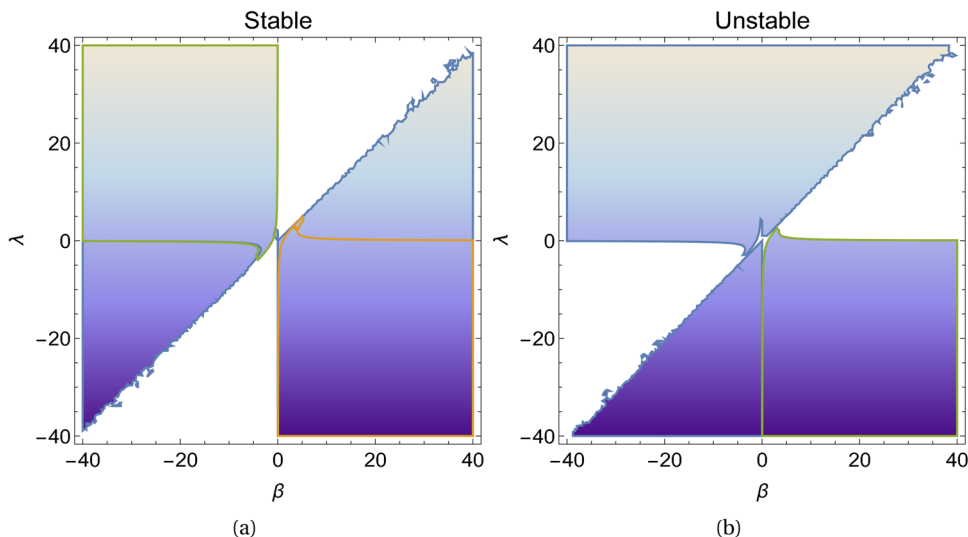
Point C is of non-hyperbolic type. Stating this, it is found that the complexity of the eigenvalues (due to higher power parameters) and the eigenvectors of the point C obstructs us from carrying out further analysis, required

to implement the Centre Manifold Theory to decide the nature of the fixed point. Thus, with a comprehensive purpose, to show the stable properties of this point we follow an analytical approach. We plot the parameter space regions for the fixed point to be stable and unstable in Fig. 1. The Fig. 1a portrays the regions of the parameter space where the point C is stable whereas the Fig. 1b portrays the regions of the parameter space where the point C exhibits instability and the intersection hyper-surface between these two regions represents the saddle surface. We now carry out further analysis for fixed-point C with the help of the Table 1. As can be seen from the Fig. 1 that at some specific regions of parameter space where ‘ λ ’ vanishes and ‘ β ’ is non-negative, the kinetic energy becomes negative and the universe exhibits phantom dominated behaviour. On the contrary, in the regions where ‘ β ’ becomes zero and ‘ λ ’ is non-negative, the kinetic term becomes canonical. Thus, in order to be dominated by the standard canonical kinetic term, the point needs to be unstable. Hence, in the ongoing case, we conclude that though the flow becomes dynamic and highly unstable, slight fluctuation will resurrect the stability. The above conclusion substantiates the choice of action surveyed in the present study, where the fusion of canonical and non-canonical scalar fields, with little fluctuation, can introduce both stability and instability dynamics for the zeroth-order background universe.

Critical point D is completely dominated by scalar field ϕ ($\Omega_\phi = 1$) in the phase-space. The point D exists for all real values of λ . For $\lambda^2 > -2$ limit, it describes an accelerating solution.

The case in which $\lambda = 0$, the scalar field (DE) behaves as cosmological constant ($\omega_{eff} = -1$). For the case

Fig. 1 The allowed range of parameter $[\beta, \lambda]$ space in which critical point C exhibits **a** stability and **b** instability characteristics



$\lambda^2 > 0$, the universe portrays phantom field dominated behavior. Whereas the case $-2 < \lambda^2 < 0$, portrays the quintessence field dominated behavior. Point D is also a non-hyperbolic type critical point. As explained in the above case for point B, the linear stability theory is not sufficient to determine its nature. Therefore, we apply the centre manifold theory to study the nature of point D.

5.2 Centre manifold theory

We now examine the stability properties of the above fixed points B and D.

Critical point B

The Jacobian matrix at the point B can be set as

$$J_B = \begin{bmatrix} -\frac{3}{2} - 3\beta^2 & 0 & -\sqrt{\frac{3}{2}}\beta & \sqrt{\frac{3}{2}}\left(\frac{1}{2} + \frac{\beta^2}{3}\right) \\ 0 & \frac{3}{2} - \beta^2 + \beta\lambda & 0 & 0 \\ \sqrt{\frac{2}{3}}\beta(3 + 2\beta^2) & 0 & 0 & -\beta\left(1 + \frac{2}{3}\beta^2\right) \\ 0 & 0 & 0 & 0 \end{bmatrix}. \tag{5.18}$$

So the eigenvalues of J_B are given as $0, -2\beta^2, -\frac{3}{2} - \beta^2, \frac{3}{2} - \beta^2 + \beta\lambda$ and the corresponding eigen vectors are $\left[\frac{1}{\sqrt{6}}, 0, \frac{-2\beta}{3}, 1\right]^T, \left[-\frac{\sqrt{6}\beta}{3+2\beta^2}, 0, 1, 0\right]^T, \left[-\frac{\sqrt{\frac{3}{2}}}{2\beta}, 0, 1, 0\right]^T$ and $[0, 1, 0, 0]^T$.

To apply centre manifold theory, we first perform coordinate transformations such that the critical point moves to the origin and the system, accordingly changing to

$$x = X - \sqrt{\frac{2}{3}}\beta, \quad y = Y,$$

$$z = Z + \left(1 + \frac{2}{3}\beta^2\right), \quad k = K.$$

Here, the parameter Ω_m is replaced with ‘z’ to ease the symbolic notation.

We bring in one more set of coordinates (x_t, y_t, z_t, k_t) in terms of (X, Y, Z, K) . By using the eigenvectors of the J_B , we insert the following new coordinate system

$$\begin{bmatrix} x_t \\ y_t \\ z_t \\ k_t \end{bmatrix} = \begin{bmatrix} \frac{\sqrt{6}\beta}{3+2\beta^2} & 0 & \frac{\sqrt{\frac{3}{2}}}{2\beta} & -\frac{1}{\sqrt{6}} \\ 0 & 1 & 0 & 0 \\ 1 & 0 & 1 & \frac{2\beta}{3} \\ 0 & 0 & 0 & 1 \end{bmatrix} \begin{bmatrix} X \\ Y \\ Z \\ K \end{bmatrix}. \tag{5.19}$$

This new coordinate system allows us to transform the autonomous system (5.2)–(5.4) and (5.6) as

$$\begin{bmatrix} x'_t \\ y'_t \\ z'_t \\ k'_t \end{bmatrix} = \begin{bmatrix} A(\beta) & 0 & 0 & 0 \\ 0 & \left(\frac{3}{2} - \beta^2 + \beta\lambda\right) & 0 & 0 \\ 0 & 0 & B(\beta) & 0 \\ 0 & 0 & 0 & 0 \end{bmatrix} \begin{bmatrix} x_t \\ y_t \\ z_t \\ k_t \end{bmatrix} + \begin{bmatrix} \text{non} \\ \text{linear} \\ \text{terms} \end{bmatrix} \tag{5.20}$$

where,

$$A(\beta) = \frac{\beta}{(-9 + 6\beta^2)} \times \left[9\sqrt{6} + 2\beta(-9 + \beta(9\sqrt{6} + 2\beta(-9 + \sqrt{6}\beta)))\right],$$

$$B(\beta) = \frac{1}{6(-3 + 2\beta^2)} \left[27 - 2\beta(9\sqrt{6} + 2\beta(-18 + \beta(9\sqrt{6} + \beta(-9 + 2\sqrt{6}\beta)))\right].$$

To find a definitive solution to these equations using standard methods is an impassable task. Thence, we make a series

expansion of $h(k_t)$ in the powers of k_t . By the definition of the centre manifold (refer to sec.2.4 of [64]), there exists a sufficiently regular function ‘h’ such that

$$\begin{bmatrix} x_t \\ y_t \\ z_t \end{bmatrix} = h(k_t) = \begin{bmatrix} a_1 k_t^2 + a_2 k_t^3 + \mathcal{O}(k_t^4) \\ b_1 k_t^2 + b_2 k_t^3 + \mathcal{O}(k_t^4) \\ c_1 k_t^2 + c_2 k_t^3 + \mathcal{O}(k_t^4) \end{bmatrix}. \tag{5.21}$$

We differentiate this with respect to ‘N’ and apply the chain rule which yields

$$\begin{bmatrix} \frac{dx_t}{dN} \\ \frac{dy_t}{dN} \\ \frac{dz_t}{dN} \end{bmatrix} = \begin{bmatrix} 2a_1 k_t + 3a_2 k_t^2 + \mathcal{O}(k_t^3) \\ 2b_1 k_t + 3b_2 k_t^2 + \mathcal{O}(k_t^3) \\ 2c_1 k_t + 3c_2 k_t^2 + \mathcal{O}(k_t^3) \end{bmatrix} \times \left[\frac{dk_t}{dN} \right] \tag{5.22}$$

where, $a_i, b_i, c_i \in \mathbb{R}$. As we analyze arbitrary small neighbourhood of the origin, we keep only lowest power terms in CMT. Comparing lowest powers of non-zero coefficients of k_t from both sides of Eq. (5.22), we deduce the solution as $a_1 = C(\beta, \Gamma)$, $b_i = 0$ and $c_1 = D(\beta, \Gamma)$ where, $C(\beta, \Gamma)$ and $D(\beta, \Gamma)$ can be interpreted from Eqs. (5.23) and (5.25) respectively.

Thus, we observe that the centre manifold given by the Eq. (5.21) can be put down as

$$\begin{aligned} x_t = & \frac{1}{6} \left(-6 - 8\Gamma_k - \frac{3}{\beta^2} - \frac{\sqrt{6}(3 + \Gamma_k)}{\beta} \right. \\ & + \frac{-6(7 + 10\Gamma_k) + 4\sqrt{6}(1 + 4\Gamma_k)\beta}{-3 + 2\beta^2} + \frac{48(6 + \sqrt{6}\beta)}{(3 - 2\beta^2)^2} \\ & + \frac{18(-1 + 2\Gamma_k)}{(3 + 2\beta^2)^2} \\ & \left. + \frac{2(6 + \sqrt{6}\beta + 2\Gamma_k(-6 + \sqrt{6}\beta))}{(3 + 2\beta^2)^2} \right) k_t^2 + \mathcal{O}(k_t^3), \end{aligned} \tag{5.23}$$

$$y_t = 0, \tag{5.24}$$

$$\begin{aligned} z_t = & \frac{1}{9} \left(6(-5 + 9\Gamma_k) - \frac{3\sqrt{6}}{\beta} - 2\sqrt{6}(7 + 4\Gamma_k)\beta \right. \\ & - \frac{3(-1 + 2\Gamma_k)(6 + \sqrt{6}\beta)}{(3 + 2\beta^2)} \\ & + \frac{6(30 - 24\Gamma_k + 15\sqrt{6}\beta) + 10\sqrt{6}\Gamma_k\beta}{(3 - 2\beta^2)} \\ & \left. - \frac{144(3 + 2\sqrt{6}\beta)}{(3 - 2\beta^2)^2} \right) k_t^2 + \mathcal{O}(k_t^3), \end{aligned} \tag{5.25}$$

and therefore, the flow on the centre manifold obtains the form as

$$\begin{aligned} \frac{dk_t}{dN} = & -2(1 - \Gamma_k)\beta k_t^2 + \frac{4\sqrt{6}(1 - \Gamma_k)\beta(3 + 2\beta^2)}{-9 + 6\beta^2} k_t^3 \\ & + \mathcal{O}(k_t^4). \end{aligned} \tag{5.26}$$

We are interested only in the non-zero coefficients of lowest power terms of k_t in CMT as we analyze an arbitrarily small neighbourhood of the origin. Accordingly, the lowest power term of the expressions of the center manifold is k_t^2 which depends upon the sign of Γ_k and β . For the defined range of $\phi : 0 \sim \pi$, the value of Γ_k does not exceed 1, and that keeps $(1 - \Gamma_k)$ a positive quantity during the complete analysis of point B. By looking at the centre manifold equations, it has been noted that an analytical approach to understand the stability and qualitative nature in the neighbourhood of the non-hyperbolic point B will be unusable, and thus, we aim to achieve the same with numerical analysis. For this purpose, we choose the different values of Γ_k and β with the already prescribed range of Γ_k . The various choices of these parameter values direct us towards the same form of the centre manifold and hence, showing the stability analysis only for one such set of values would be enough to understand its behaviour on the center manifold near the origin. For the chosen value of $\beta = \pm 0.5$ and $\Gamma_k = -1$ the stability analysis follows as:

If $\beta > 0$ then the origin becomes a saddle node and it is unstable. This signals that the local phase portrait is as given by Fig. 2a. The behaviour of the vector field near the origin and the flow on the centre manifold in the $z_t - k_t$ plane is the same as Fig. 2a. If $\beta < 0$ then the local phase portrait is as given by Fig. 2b, c for $x_t - k_t$ and $z_t - k_t$ planes respectively. We detect that the origin is a saddle node and hence it is unstable in nature. The topological equivalence makes the behaviour of the non-hyperbolic point B in the old coordinate system similar to the behaviour of the centre manifold in the vicinity of the origin in the new coordinate system and that it is unstable due to its saddle nature.

Critical point D

The Jacobian matrix at the point D can be set as

$$J_D = \begin{bmatrix} -3 - \lambda^2 - \frac{\lambda}{2}\sqrt{6 + \lambda^2} & -\sqrt{\frac{3}{2}}\beta & 0 \\ 0 & -3 - \frac{\lambda^2}{2} & 0 \\ 0 & 0 & (-3 - \lambda^2 + \beta\lambda) \\ 0 & 0 & 0 \end{bmatrix}. \tag{5.27}$$

So the eigenvalues of J_D are given as $0, -3 - \frac{\lambda^2}{2}, -3 - \lambda^2 + \beta\lambda$, and the corresponding eigen vectors are $[1, 0, 0, 0]^T, [-\sqrt{1 + \frac{6}{\lambda^2}}, 1, 0, 0]^T, [-\sqrt{\frac{3}{2\lambda^2}}, 0, 1, 0]^T$ and $[0, 0, 0, 1]^T$.

We, now modify the coordinates such that the critical point moves to the origin and the system, correspondingly changes to

$$x = X - \frac{\lambda}{\sqrt{6}}, \quad y = Y + \sqrt{1 + \frac{\lambda^2}{6}}, \quad z = Z, \quad k = K.$$

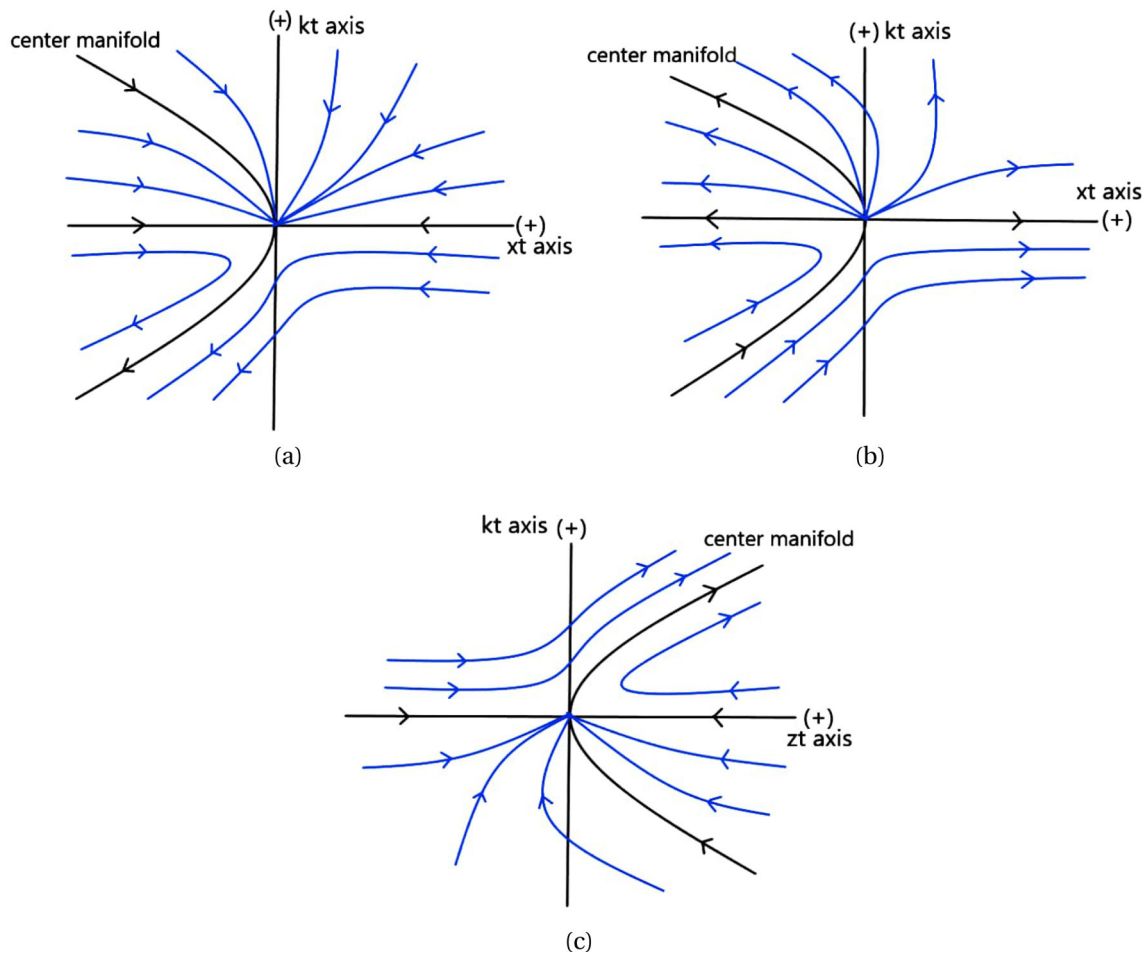


Fig. 2 The phase portrait in the proximity of the origin for the critical point B. **a** Represents the vector field near the origin in $x_t - k_t$ plane for $\beta > 0$. **b** and **c** respectively, represent the vector field near the origin in

$x_t - k_t$ and $z_t - k_t$ plane for $\beta < 0$. The arrows indicate the flow along the center manifold (black curve)

Here as well, the parameter Ω_m is replaced with ‘z’ to ease the symbolic notation.

Subsequently, settling the similar arguments as implemented in the above case, we understand that the centre manifold, in this case too, is given as

$$x_t = 0, \tag{5.28}$$

$$y_t = 0, \tag{5.29}$$

$$z_t = 0, \tag{5.30}$$

and thus, making the flow on the centre manifold vanish as

$$\frac{dk_t}{dN} = 0. \tag{5.31}$$

In this event, the data is not adequate to know the stability properties of point D near the origin. So, a bit different from the above analysis, we attempt to picture the stability of the vector field near the origin on each plane. The stability properties of the vector field on each plane for point D are shown in Table 3. In the table, we denote, $c = \beta\lambda - \lambda^2$.

In the following subsection, we exhibit the graphical representation of the above qualitative analysis of the critical points with constraints on the DE–DM interaction model.

5.3 Constraints on DE–DM interaction model

The specified form of potential has already simplified the analysis of an autonomous system for coupled DE–DM model. However, it has been observed that at late times, the cosmological parameters show nearly steady behaviour with ‘ $\ln(a)$ ’ variation (the reader can also refer [63]). This supposition brings us a practicability to constrain the model in such a way that the term ‘ $\left(\frac{2\beta-k}{2}\right)\Omega_m$ ’ in the interaction strength obtained in Eq. (5.11) becomes a constant (C) entity. Here, we define ‘C’ as a coupling constant. For further analysis of the phase-space portrait, the choice of the potential and other parameter values are as mentioned in Eq. (5.32). The physical motivation behind choosing such set of parameters is that they facilitate the universe’s current cosmological evolution.

Table 3 Stability properties of vector field for critical point D

Coordinate plane	Stability
$x_t y_t$	Vector field is stable about x_t axis for any real value of λ
$x_t z_t$	For $-3 < -c$, vector field is stable about x_t axis, for $-3 > -c$, vector field is unstable about x_t axis, for $c = 3$, vector fields are nearly parallel to x_t axis and obeys stability behaviour about k_t axis as shown in the Fig. 3. In the plot the tracking nature of solutions running from higher z_t to lower z_t values is observed
$x_t k_t$	Vector field is stable about x_t axis for any value of λ
$y_t z_t$	For $-3 < -c$, vector field near the origin is a stable node, for $-3 > -c$, vector field near the origin is a saddle node, for $c = 3$, vector field is stable about z_t axis
$y_t k_t$	Vector field near the origin acts as stable star for any real value of λ
$z_t k_t$	For $-3 < -c$, vector field near the origin is a stable node, for $-3 > -c$, vector field near the origin is a saddle node, for $c = 3$, vector field is stable about z_t axis

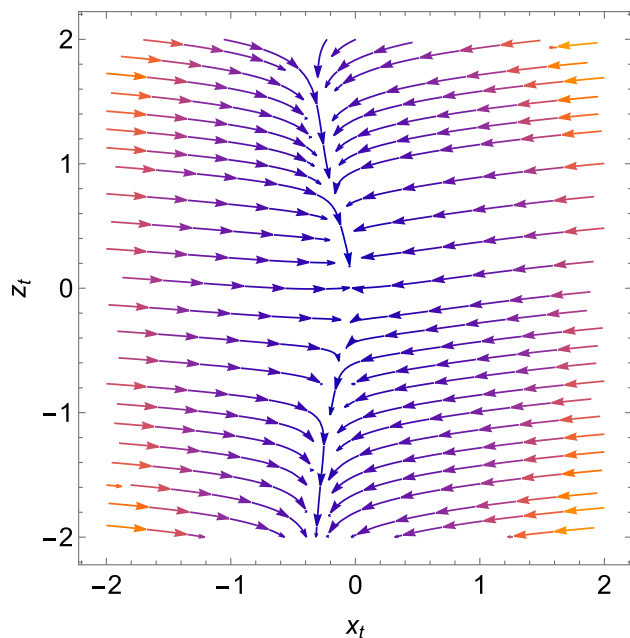


Fig. 3 Vector field projection on $x_t z_t$ coordinate plane when $c = 3$ for fixed point D for $\lambda = 0.5$ and coupling constant ‘C’ = 0.04

$$\begin{aligned}
 V(\phi) &= V_0 e^{\alpha(\phi)}, \quad B(\phi) = \sin^2(\phi), \quad k(\phi) = -2c \cot(\phi), \\
 \alpha(\phi) &= c' \phi, \quad \beta = -\frac{c'}{\alpha},
 \end{aligned}
 \tag{5.32}$$

where ‘ ϕ ’ varies between 0 and π . We show the cosmological evolution for positive values of coupling constant(C). Figure 4 represents the plots for the evolution of the relative density parameter of DE and DM as a function of ‘N’ for different values of coupling constant. The plots clearly show the DM dominated universe over a long period of time in the past and then evolve to the DE field(ϕ) dominated universe. Figure 4a portrays uncoupled case and the behaviour becomes analogous to the canonical scalar field. Figure 4b portrays the behaviour for the coupling constant ‘C’ = 0.04. For such smaller coupling strengths, we get a completely viable back-

ground cosmological model. Figure 4c indicates the onset of negative dark energy density parameter for ‘C’ = 0.07 which can clearly be seen in Fig. 4d for further higher values of ‘C’. We found that for coupling strength ‘C’ > 0.07, the DE density parameter violates the WEC in the past thus, setting an upper bound of ‘C’ = 0.07 for $\lambda = 1$. The other allowed values of λ would make no difference on the upper limit value. Thus, looking at the results we emphasize that the said violation could be avoided and the current background dynamics obeying the energy condition (WEC) can be achieved by pertaining to the small ‘C’ values. Hence, we follow the smaller couplings to avoid any other such ambiguities. For coupling constant(C)=0.04, Fig. 4b mirrors the current observational measurements of DE and DM density in the present-day observable universe.¹ This may equip us with derived empirical results of the coincidence problem. Also, we have observed that for allowed ‘C’ values, the results are compatible with the current evolution of the dark energy EoS parameter, “ ω_ϕ ” (Fig. 7), the effective EoS parameter, “ ω_{eff} ” (Fig. 8a) and Hubble parameter, “H” (Fig. 8b), respectively (refer [85–92] and references therein).

The observation of Fig. 5 suggests that the density parameter Ω_m changes steadily at late times. Also, to ease the analysis of the system, we select some particular values of the parameter ‘k’ along with ‘ β ’ where the coupling term $\frac{(2\beta-k)}{2} \Omega_m$ takes values as C = 0, C = 0.005, C = 0.04. We are interested in positive values of coupling strength² and hence the analysis has been performed only for those values.

Our focus on the late-time cosmological behavior of the universe makes this feature agreeable to examining the time evolution of variables x and y in Fig. 6. We observe the dark energy dominated solution for a coupled DE–DM model for critical point D represented by a red dot in Fig. 6. All the trajectories moving towards point D signals the stable attractor

¹ The dominance of the dark energy over the dark matter takes place at later time if we further lower the “ λ ” value.

² The negative coupling constant produces approximately same results (the reader can refer [63]).

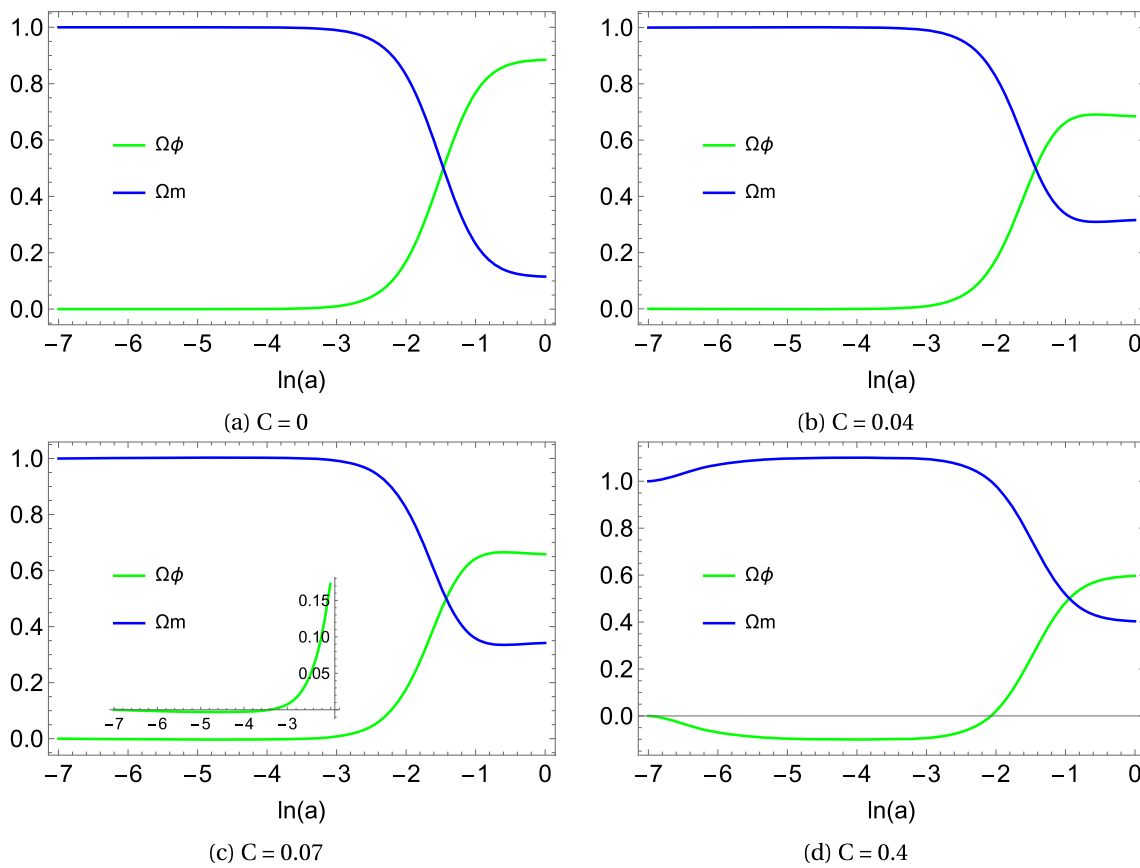


Fig. 4 The relative density parameter of DE (Ω_ϕ) and DM (Ω_m) with varying $N = \ln(a)$ for various values of coupling constant (C)

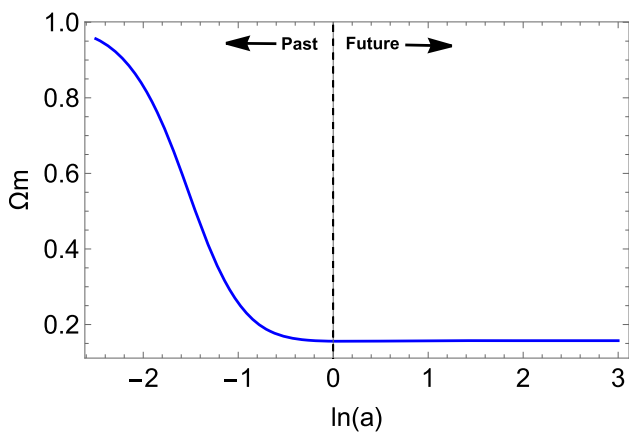


Fig. 5 Late time evolution of DM energy density for an interacting DE–DM model

nature of the critical point and the figure exhibits an everlasting late-time accelerated nature of the universe for $\lambda^2 > -2$. The phase space portraits are shown for different values of λ and thus, we reveal that regardless of the initial conditions the qualitative behavior of the universe at the background level nearly remains the same. It can also be spotted that all the trajectories are getting attracted towards a single tra-

jectory and not crossing that specific one. These dynamics urge us to proclaim that trajectory itself, in this incident, is acting as an attractor. We call them a late-time acceleration trajectory similar to an inflationary trajectory (separatrix) in an inflationary scenario.

Figure 7 presents the cosmological evolution of DE EoS parameter. It can be seen that in recent times, the dynamics of the evolution are dominated by the DE field “ ϕ ”. We extrapolate that the behaviour corresponds to phantom regime. On the other hand, the dynamics of the effective EoS parameter, ω_{eff} tracks the quintessence dominated nature “ $-1 < \omega_{eff} < -\frac{1}{3}$ ” to phantom dominated nature “ $\omega_{eff} < -1$ ” in the present time (Fig. 8a). Hence, the analysis clearly signifies the present time accelerated expansion of the universe.

Furthermore, from the Fig. 7a it can be seen that ω_ϕ attains larger negative values at the onset of the dark energy component domination. This feature results from the coupling effect on the ω_ϕ behaviour. If we reduce the coupling, the ω_ϕ becomes less negative (see Fig. 7c, d) as permitted by the observations [69,93–95]. (Also, It is found that small coupling “ C ” have minimal effect on the evolution of density parameters (refer Fig. 9a)). And if we further increase the

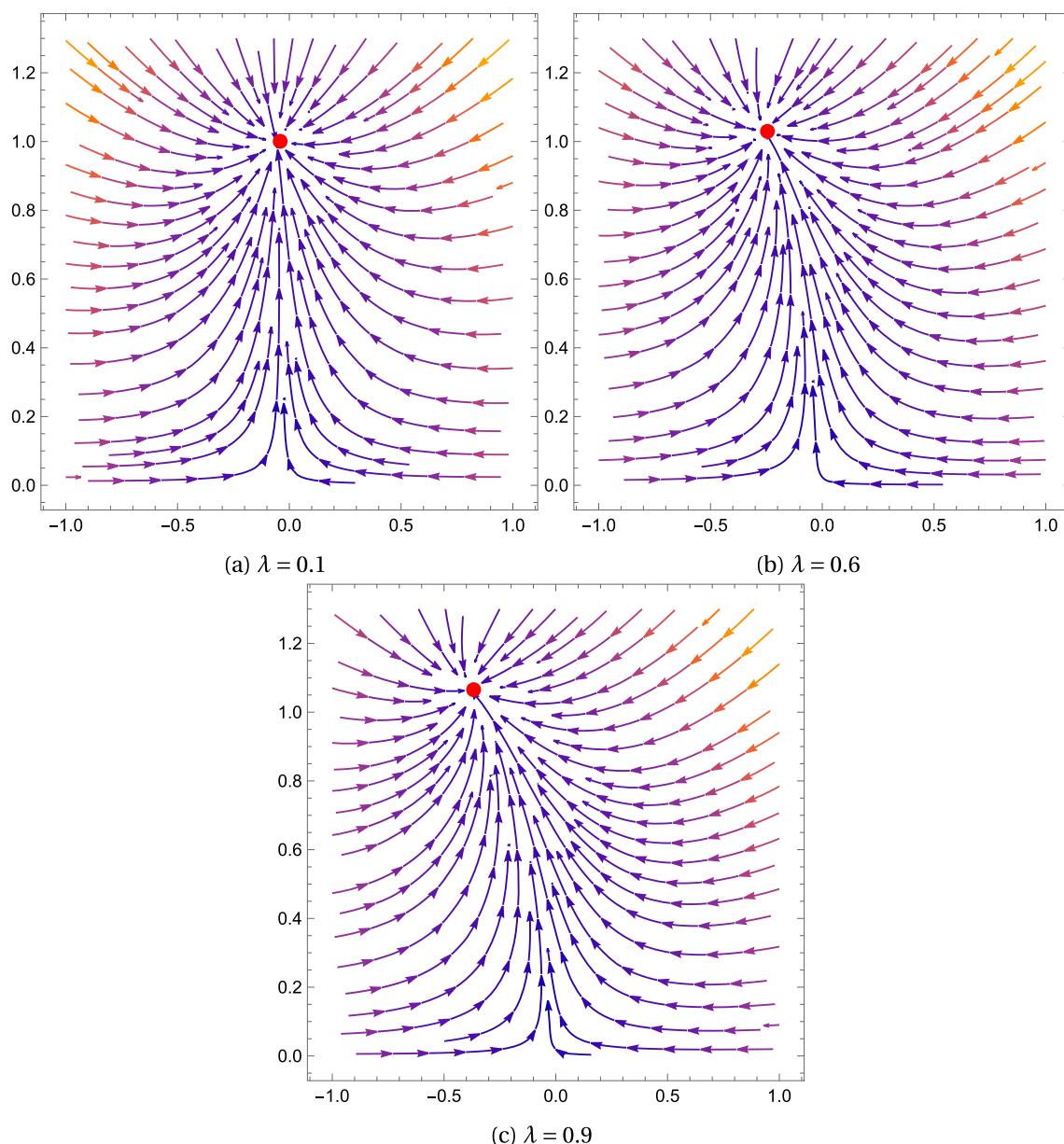


Fig. 6 The phase space portraits of the dynamical system for an equilibrium point D for $\lambda = 0.1$, $\lambda = 0.6$ and $\lambda = 0.9$ with a coupling constant ‘C’ = 0.04. The horizontal axis represents variable ‘x’ and vertical axis represents variable ‘y’

“C”³, the feature remains the same (with large negative value) but gets shift in the future (Fig. 7b). With this knowledge in mind, we find from the Fig. 9 that there is no appearance of singularity even in the far future regardless of the size of the coupling. All these findings are based upon the consideration that whether introduction of interaction and by how much amount causes any type of singularity or not. Here,

³ Here, we found that dark energy do not overtake the dark matter for large “C” values which is not physically acceptable scenario. Therefore, we restrict the coupling to be minimal to achieve the necessary dynamics. Nevertheless, these dynamics again depend upon the constraint put on the parameter “ λ ”.

we have observed that irrespective of the coupling considered, the behaviour of ω_ϕ stabilizes at ~ -1 at present time (see Fig. 7). Thus, in our investigation we find with the constraints on this EoS parameter that, this particular model of interaction between dark matter and dark energy gives rise to the accelerated expansion of the universe at late times and can also help to avoid the possibility of big rip singularity (if there is any in the future) since EoS parameter always tends towards -1 ($\omega_\phi \rightarrow -1$) in the present time and even in the

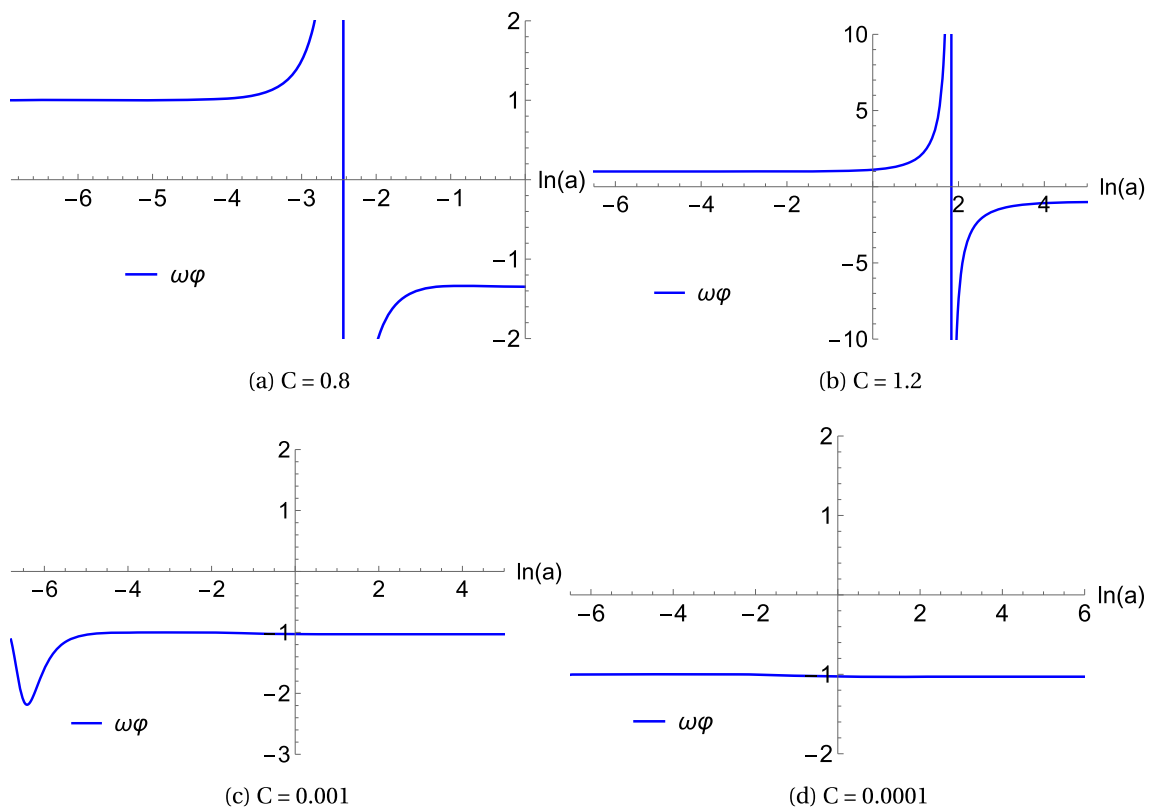


Fig. 7 The qualitative behaviour of the DE equation of state (ω_ϕ) parameter for different values of coupling constant (C)

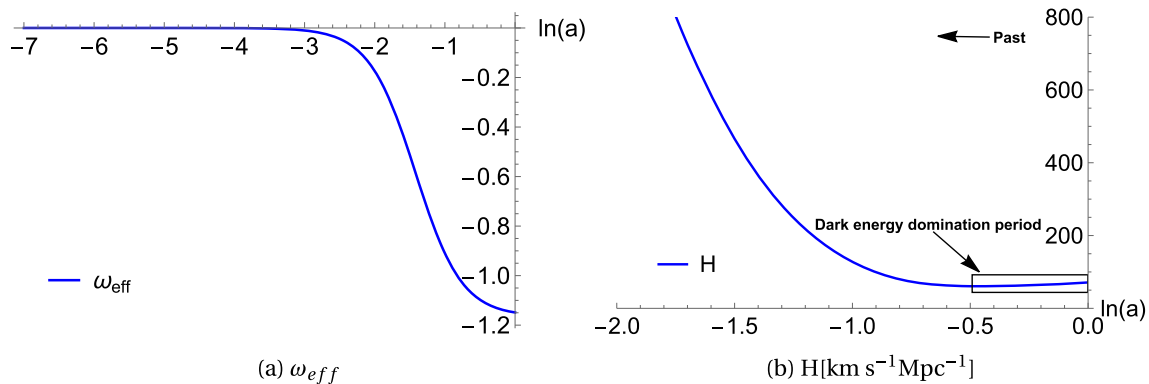


Fig. 8 The evolution of the effective equation of state parameter (ω_{eff}) and the Hubble parameter (H) as a function of $N = \ln(a)$ for an interacting DE–DM model

future (Fig. 7), giving us an attractor de Sitter like solution on the large scale.⁴

To summarize, the constraints on the proposed DE–DM interaction model restrict the potential and the values of other parameters facilitating the currently observed evolution of the universe, as shown in [24,84,96]. The dynamical stability analysis and the analysis from Figs. 4, 5, 6, 7 and 8 suggest that with the appropriate choice of parameters β and λ , the universe exhibits DM dominated nature long enough to let the

structure formations to happen. Later, it evolves to DE (field ‘ ϕ ’) dominated universe causing an accelerated expansion in agreement with the current cosmological observations.

6 Conclusions

In this article, we have put forward the representation of the two-field dark sector model to describe the accelerated expanding universe and also to test the feasibility of the model in the background cosmology under the convenience of chi-

⁴ This has already been investigated in this study.

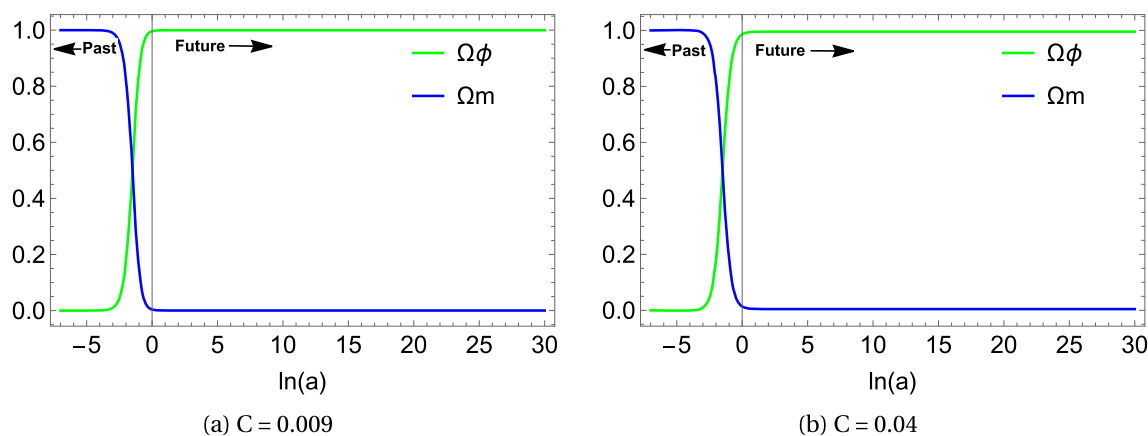


Fig. 9 The variation of density parameter Ω_ϕ and Ω_m for couplings $C = 0.009$ and $C = 0.04$ exhibiting no appearance of future singularity

ral cosmology. We set up a general formulation method to study 2-field chiral model. Further, approaching this point of view, to study the dark sector fields' evolution. We proposed an interacting canonical and non-canonical scalar field model termed as coupled DE–DM model. We presented that there is a resemblance between the field theory approach and phenomenological fluid approach to study the DE–DM interaction model. This method makes all the cosmological equations appear in terms of DM fluid and DE scalar field ϕ , creating possible scenarios to formulate the dynamical system of equations effortlessly. In our case, we have opted not to surplus the system of equations signaling the radiation-dominated era and thus, focused on the dark matter and dark energy dominated period of the universe. We chose this scenario since we are interested in studying the late time cosmological behaviour.

Later, we conducted a detailed fixed point analysis and stability analysis of the dynamical system set up for an interacting DE–DM model. The chosen exponential potential of the form $V(\phi) = V_0 e^{\alpha(\phi)}$ and parameters constraints reduced the dimensions of the system to make further analysis even more comfortable. The critical points obtained are of non-hyperbolic nature. However, the linear stability theory can still be employed to decide the nature of the points A, B, and D but vaguely. On the other hand, point C contains cosmological parameters of higher power terms and the stability analysis is found to be convoluted.

For the critical point A, we have gained parameter restrictions to be $\Gamma_k < 1$ indicates the saddle nature of the point but $\Gamma_k > 1$ leaves the stability undetermined. Also, the vanishing ω_{eff} makes this point unsuitable for acceleration. The critical point B has been analysed with the employment of the centre manifold theory and its stability features have correspondingly been portrayed in Fig. 2. Point B describes both quintessence and phantom DE dominated accelerated expansion as seen from Table 1. The cosmological evolution cor-

responding to point C describes the scaling solution and also describes an accelerated era of the universe for parameters with $-2 < \frac{\lambda}{\beta} < 1$ constraint. It is to be noted that for vanishing $\frac{\lambda}{\beta}$, point C nurtures the de Sitter universe. The point gains the cosmological importance since the late time accelerated scaling solution can alleviate the coincidence problem as well with few constraints on parameters. The Fig. 1 facilitate us with the allowed range of parameters to understand the stable and unstable behaviour of point C accordingly. The non-hyperbolic critical point D also exhibits an accelerating universe under $\lambda^2 > -2$ parameter constraint. Point D has been analysed with the application of the centre manifold theory and its stability features are corresponding as shown in Table 3. For specific values of parameter λ , the point is a stable attractor (Fig. 6) and describes the cosmological constant or phantom field or quintessence field dominated universe.

To complement the above analysis, in our work, we have also discussed the graphical presentation of the dynamical system. In Fig. 4 we studied the evolution of density parameters of dark matter and dark energy. We set our analysis to be short of radiation component supposing that the universe has encountered a radiation dominated era long before it evolved to the time period dominated by the dark matter which is in late time follows the dark energy dominated behaviour as it is seen from Fig. 4. Figure 5 shows the era where the evolution of dark matter energy density becomes almost constant after it went through an era that is long enough for all kinds of structure formation to take place. Later we discussed the phase-space portrait of the system (Fig. 6) picturing the stable attractor D determining the late time DE dominated accelerated evolution of the universe. The evolution of the equation of state parameters in Figs. 7 and 8a also shows cosmologically relevant behaviour complimenting the afore-said analysis of the dynamical system. This investigation also implies that the occurrence of future singularity problem is absent and even if there is any it can be cured.

The above analysis suggests that Chiral cosmological theory can be used to sense the cosmologically viable solutions in the realm of background dynamics, where we notice a sufficiently long, extended era of the matter-dominated universe to an era of an accelerated expanding universe in the present time. Our next plan is to employ the observational data analysis methods and be more precise about the parameter values encountered in the current study. In the future, we also plan to investigate other relevant cosmological models [97–100] under the Chiral theory of cosmology and also plan to analyze them by bringing in the cosmological experimental framework.

Acknowledgements This work is partially supported by DST (Govt. of India) Grant No. SERB/PHY/2021057.

Data Availability Statement This manuscript has no associated data or the data will not be deposited. [Authors’ comment: No observational data is used for this analysis.]

Open Access This article is licensed under a Creative Commons Attribution 4.0 International License, which permits use, sharing, adaptation, distribution and reproduction in any medium or format, as long as you give appropriate credit to the original author(s) and the source, provide a link to the Creative Commons licence, and indicate if changes were made. The images or other third party material in this article are included in the article’s Creative Commons licence, unless indicated otherwise in a credit line to the material. If material is not included in the article’s Creative Commons licence and your intended use is not permitted by statutory regulation or exceeds the permitted use, you will need to obtain permission directly from the copyright holder. To view a copy of this licence, visit <http://creativecommons.org/licenses/by/4.0/>.

Funded by SCOAP³. SCOAP³ supports the goals of the International Year of Basic Sciences for Sustainable Development.

Appendix

Since the output corresponding to eigenvalues of critical point C is too big to handle and it is a tedious task to display them on the full scale, we struck out a large number of terms and simply intended to disclose the mannerism in which it appears during the course of action which makes them inconvenient to deploy for the analysis of stability behaviour of the corresponding fixed point.

$$\left[0, \frac{1}{(\beta - \lambda)^4} \sqrt{(2592\beta^9 - 1728\beta^{11})(\beta - \lambda) - 5760\beta^{11}(\beta - \lambda)\lambda^2 + \dots + (96\beta^9\lambda + \dots)}, \right. \\ \left. \frac{1}{(\beta - \lambda)^4} \sqrt{-1728\beta^{11}(\beta - \lambda) + (20736\beta^8\lambda + 72576\beta^7\lambda^2)(\beta - \lambda) + \dots + (72\beta^6\lambda^2 + \dots)}, \right. \\ \left. \frac{1}{(\beta - \lambda)^4} \sqrt{-1728\beta^{11}(\beta - \lambda) + \dots - 10368(\beta - \lambda)\beta^4\lambda^7 + (96\beta^9\lambda + \dots - 1296\beta\lambda^5) + \dots} \right].$$

References

1. S. Perlmutter, G. Aldering et al., Discovery of a supernova explosion at half the age of the universe. *Nature* **391**, 51–54 (1998)
2. S. Perlmutter, G. Aldering, G. Goldhaber et al., Measurements of Ω and Λ from 42 high-redshift supernovae. *Astrophys. J.* **517**, 565–586 (1999)
3. A.G. Riess, A.V. Filippenko et al., Observational evidence from supernovae for an accelerating universe and a cosmological constant. *Astron. J.* **116**, 1009–1038 (1998)
4. A.G. Riess, R.P. Kirshner et al., *BVRi* light curves for 22 type Ia supernovae. *Astron. J.* **117**, 707–724 (1999)
5. J. Dunkley, E. Komatsu, M.R. Nolta et al., Five-year Wilkinson microwave anisotropy probe observations: likelihoods and parameters from the WMAP data. *Astrophys. J. Suppl. Ser.* **180**, 306–329 (2009)
6. S.P. Boughn, R.G. Crittenden, A detection of the integrated Sachs–Wolfe effect. *New Astron. Rev.* **49**, 75–78 (2005)
7. D.J. Eisenstein, I. Zehavi et al., Detection of the baryon acoustic peak in the large-scale correlation function of SDSS luminous red galaxies. *Astrophys. J.* **633**, 560–574 (2005)
8. M. Tegmark, M.A. Strauss et al., Cosmological parameters from SDSS and WMAP. *Phys. Rev. D* **69**, 103501 (2004)
9. W.J. Percival, S. Cole, D.J. Eisenstein et al., Measuring the baryon acoustic oscillation scale using the Sloan Digital Sky Survey and 2dF galaxy redshift survey. *Mon. Not. R. Astron. Soc.* **381**, 1053–1066 (2007)
10. M. Tegmark, D.J. Eisenstein, M.A. Strauss et al., Cosmological constraints from the SDSS luminous red galaxies. *Phys. Rev. D* **74**, 123507 (2006)
11. E. Di Valentino, A. Melchiorri, O. Mena, S. Vagnozzi, Nonminimal dark sector physics and cosmological tensions. *Phys. Rev. D* **101**(6), 063502 (2020)
12. E.J. Copeland, M. Sami, S. Tsujikawa, Dynamics of dark energy. *Int. J. Mod. Phys. D* **15**, 1753–1935 (2006)
13. L. Amendola, S. Tsujikawa, in *Dark Energy: Theory and Observations*, ed. by L. Amendola, S. Tsujikawa (Cambridge University Press, Cambridge, 2010). ISBN:9780521516006
14. O. Lahav, Dark energy: is it just Einstein’s cosmological constant Λ ? *Contemp Phys* **61**, 132–145 (2020)
15. S. Weinberg, The cosmological constant problem. *Rev. Mod. Phys.* **61**, 1–23 (1989)
16. M. Doran, C. Wetterich, Quintessence and the cosmological constant. *Nucl. Phys. B Proc. Suppl.* **124**, 57–62 (2003)
17. B. Wang, E. Abdalla, F. Atrio-Barandela, D. Pavón, Dark matter and dark energy interactions: theoretical challenges, cosmological implications and observational signatures. *Rep. Prog. Phys.* **79**, 096901 (2016)

18. I. Zlatev, L. Wang, P.J. Steinhardt, Quintessence, cosmic coincidence, and the cosmological constant. *Phys. Rev. Lett.* **82**, 896–899 (1999)
19. H.E.S. Velten, R.F. vom Martens, W. Zimdahl, Aspects of the cosmological “coincidence problem”. *Eur. Phys. J. C* **74**(11), 3160 (2014)
20. Sd. Campo, R. Herrera, D. Pavón, Interacting models may be key to solve the cosmic coincidence problem. *J. Cosmol. Astropart. Phys.* **2009**, 020 (2009)
21. M. Bouhmadi-López, J. Morais, A. Zhuk, The late universe with non-linear interaction in the dark sector: the coincidence problem. *Phys. Dark Universe* **14**, 11–20 (2016)
22. R. Potting, P.M. Sá, Coupled quintessence with a generalized interaction term. *Int. J. Mod. Phys. D* **31**(15), 2250111 (2022)
23. T. Harko, F.S.N. Lobo, M.K. Mak, Arbitrary scalar-field and quintessence cosmological models. *Eur. Phys. J. C* **74**, 1–17 (2014)
24. G. Mandal, S. Chakraborty, S. Mishra, S.K. Biswas, Dynamical analysis of interacting non-canonical scalar field model (2021)
25. A. Paliathanasis, G. Leon, Dynamics of a two scalar field cosmological model with phantom terms. *Class. Quantum Gravity* **38**, 075013 (2021)
26. P.F. González-Díaz, Cosmological models from quintessence. *Phys. Rev. D* **62**, 023513 (2000)
27. T. Duary, A. Dasgupta, N. Banerjee, Thawing and freezing quintessence models: a thermodynamic consideration. *Eur. Phys. J. C* **79**(11), 888 (2019)
28. C. Armendariz-Picon, V. Mukhanov, P.J. Steinhardt, Essentials of k-essence. *Phys. Rev. D* **63**, 103510 (2001)
29. A. Sen, Tachyon dynamics in open string theory. *Int. J. Mod. Phys. A* **20**, 5513–5656 (2005)
30. K. Bamba, S. Capozziello, S. Nojiri, S.D. Odintsov, Dark energy cosmology: the equivalent description via different theoretical models and cosmography tests. *Astrophys. Space Sci.* **342**, 155–228 (2012)
31. M. Vijaya Santhi, T. Chinnappalanaidu, Rényi holographic dark energy model in a scalar–tensor theory. *New Astron.* **92**, 101725 (2022)
32. L. Susskind, The world as a hologram. *J. Math. Phys.* **36**, 6377–6396 (1995)
33. B. Feng, X. Wang, X. Zhang, Dark energy constraints from the cosmic age and supernova. *Phys. Lett. B* **607**(1), 35–41 (2005)
34. S.M. Carroll, A. De Felice, V. Duvvuri, D.A. Easson, M. Trodden, M.S. Turner, Cosmology of generalized modified gravity models. *Phys. Rev. D* **71**, 063513 (2005)
35. A.I. Lonappan, S. Kumar, Ruchika, B.R. Dinda, A.A. Sen, Bayesian evidences for dark energy models in light of current observational data. *Phys. Rev. D* **97**, 043524 (2018)
36. A. Rozas-Fernández, Kinetic k-essence ghost dark energy model. *Phys. Lett. B* **709**(4), 313–321 (2012)
37. M.P. Dąbrowski, Phantom dark energy and its cosmological consequences, in *The Eleventh Marcel Grossmann Meeting* (2008), pp. 1761–1763
38. S. Capozziello, Ruchika, A.A. Sen, Model-independent constraints on dark energy evolution from low-redshift observations. *Mon. Not. R. Astron. Soc.* **484**, 4484–4494 (2019)
39. B.-H. Lee, W. Lee, E.Ó. Colgáin, M. Sheikh-Jabbari, S. Thakur, Is local H_0 at odds with dark energy EFT? *J. Cosmol. Astropart. Phys.* **2022**, 004 (2022)
40. A. Banerjee, H. Cai, L. Heisenberg, E.Ó. Colgáin, M. Sheikh-Jabbari, T. Yang, Hubble sinks in the low-redshift swampland. *Phys. Rev. D* **103**, 081305 (2021)
41. V.K. Oikonomou, N. Chatzarakis, The phase space of k -essence $f(R)$ gravity theory. *Nucl. Phys. B* **956**, 115023 (2020)
42. J. Morais, M. Bouhmadi-López, K.S. Kumar, J. Marto, Y. Tavakoli, Interacting 3-form dark energy models: distinguishing interactions and avoiding the little sibling of the big rip. *Phys. Dark Universe* **15**, 7–30 (2017)
43. S. Chakraborty, S. Mishra, S. Chakraborty, A dynamical system analysis of cosmic evolution with coupled phantom dark energy with dark matter. *Int. J. Mod. Phys. D* **31**(01), 2150129 (2022)
44. Z.-K. Guo, R.-G. Cai, Y.-Z. Zhang, Cosmological evolution of interacting phantom energy with dark matter. *J. Cosmol. Astropart. Phys.* **2005**, 002 (2005)
45. S. Chakraborty, S. Mishra, S. Chakraborty, Dynamical system analysis of three-form field dark energy model with baryonic matter. *Eur. Phys. J. C* **80**(9), 852 (2020)
46. D. Samart, B. Silasan, P. Channuie, Cosmological dynamics of interacting dark energy and dark matter in viable models of $f(r)$ gravity. *Phys. Rev. D* **104**, 063517 (2021)
47. G. Caldera-Cabral, R. Maartens, L.A. Urena-Lopez, Dynamics of interacting dark energy. *Phys. Rev. D* **79**, 063518 (2009)
48. S. Pan, G.S. Sharov, A model with interaction of dark components and recent observational data. *Mon. Not. R. Astron. Soc.* **472**, 4736–4749 (2017)
49. S. Pan, S. Bhattacharya, S. Chakraborty, An analytic model for interacting dark energy and its observational constraints. *Mon. Not. R. Astron. Soc.* **452**, 3038–3046 (2015)
50. S.D. Odintsov, V.K. Oikonomou, P.V. Tretyakov, Phase space analysis of the accelerating multifluid Universe. *Phys. Rev. D* **96**(4), 044022 (2017)
51. V.K. Oikonomou, Classical and loop quantum cosmology phase space of interacting dark energy and superfluid dark matter. *Phys. Rev. D* **99**(10), 104042 (2019)
52. S.D. Odintsov, V.K. Oikonomou, Dynamical systems perspective of cosmological finite-time singularities in $f(R)$ gravity and interacting multifluid cosmology. *Phys. Rev. D* **98**(2), 024013 (2018)
53. P. Rudra, Towards a possible solution for the coincidence problem: $f(G)$ gravity as background. *Int. J. Mod. Phys. D* **24**(02), 1550013 (2014)
54. T. Vinutha, K. Sri Kavya, K. Niharika, Bianchi type cosmological models in modified theory with exponential functional form. *Phys. Dark Universe* **34**, 100896 (2021)
55. T. Clifton, P.G. Ferreira, A. Padilla, C. Skordis, Modified gravity and cosmology. *Phys. Rep.* **513**, 1–189 (2012)
56. A. Paliathanasis, G. Leon, S. Pan, Exact solutions in chiral cosmology. *Gen. Relativ. Gravit.* **51**(9), 106 (2019)
57. A. Paliathanasis, Dynamics of chiral cosmology. *Class. Quantum Gravity* **37**, 195014 (2020)
58. S.V. Chervon, Chiral cosmological models: dark sector fields description. *Quant. Matt.* **2**, 71–82 (2013)
59. A. Paliathanasis, G. Leon, Asymptotic behavior of N -fields chiral cosmology. *Eur. Phys. J. C* **80**(9), 847 (2020)
60. Y.-F. Cai, E.N. Saridakis, M.R. Setare, J.-Q. Xia, Quintom cosmology: theoretical implications and observations. *Phys. Rep.* **493**, 1–60 (2010)
61. K. Nozari, N. Behrouz, An interacting dark energy model with nonminimal derivative coupling. *Phys. Dark Universe* **13**, 92–110 (2016)
62. R. Lazkoz, G. Leon, Quintom cosmologies admitting either tracking or phantom attractors. *Phys. Lett. B* **638**, 303–309 (2006)
63. J.P. Johnson, S. Shankaranarayanan, Cosmological perturbations in the interacting dark sector: mapping fields and fluids. *Phys. Rev. D* **103**, 023510 (2021)
64. S. Bahamonde, C.G. Böhrer et al., Dynamical systems applied to cosmology: dark energy and modified gravity. *Phys. Rept.* **775–777**, 1–122 (2018)
65. A. Paliathanasis, G. Leon, Dynamics of a two scalar field cosmological model with phantom terms. *Class. Quantum Gravity* **38**(7), 075013 (2021)

66. L.R. Díaz-Barrón, A. Espinoza-García, S. Pérez-Payán, J. Socorro, Anisotropic chiral cosmology: exact solutions. *Int. J. Mod. Phys. D* **30**(11), 2150080 (2021)
67. R. Caldwell, A phantom menace? Cosmological consequences of a dark energy component with super-negative equation of state. *Phys. Lett. B* **545**(1), 23–29 (2002)
68. J.-G. Hao, X.-Z. Li, Phantom with Born–Infeld type Lagrangian. *Phys. Rev. D* **68**, 043501 (2003)
69. P. Singh, M. Sami, N. Dadhich, Cosmological dynamics of a phantom field. *Phys. Rev. D* **68**, 023522 (2003)
70. S. Hannestad, E. Mortsell, Probing the dark side: constraints on the dark energy equation of state from CMB, large scale structure and Type Ia supernovae. *Phys. Rev. D* **66**, 063508 (2002)
71. A. Melchiorri, L. Mersini-Houghton, C.J. Odman, M. Trodden, The state of the dark energy equation of state. *Phys. Rev. D* **68**, 043509 (2003)
72. J.A.S. Lima, J.V. Cunha, J.S. Alcaniz, Constraining the dark energy with galaxy clusters x-ray data. *Phys. Rev. D* **68**, 023510 (2003)
73. U. Alam, V. Sahni, A.A. Starobinsky, The case for dynamical dark energy revisited. *JCAP* **06**, 008 (2004)
74. U. Alam, V. Sahni, T.D. Saini, A.A. Starobinsky, Is there supernova evidence for dark energy metamorphosis? *Mon. Not. R. Astron. Soc.* **354**, 275 (2004)
75. Y. Wang, P. Mukherjee, Model-independent constraints on dark energy density from flux-averaging analysis of type Ia supernova data. *Astrophys. J.* **606**, 654–663 (2004)
76. J. Santos, J.S. Alcaniz, M.J. Rebouças, Energy conditions and supernovae observations. *Phys. Rev. D* **74**, 067301 (2006)
77. S.M. Carroll, M. Hoffman, M. Trodden, Can the dark energy equation-of-state parameter w be less than -1 ?. *Phys. Rev. D* **68**, 023509 (2003)
78. M. Visser, C. Barcelo, Energy conditions and their cosmological implications, in *3rd International Conference on Particle Physics and the Early Universe* (2000), pp. 98–112
79. J.D. Barrow, String-driven inflationary and deflationary cosmological models. *Nucl. Phys. B* **310**(3), 743–763 (1988)
80. S. Nojiri, S.D. Odintsov, S. Tsujikawa, Properties of singularities in the (phantom) dark energy universe. *Phys. Rev. D* **71**, 063004 (2005)
81. M. Sami, A. Toporensky, Phantom field and the fate of universe. *Mod. Phys. Lett. A* **19**, 1509 (2004)
82. A.V. Astashenok, S. Nojiri, S.D. Odintsov, A.V. Yurov, Phantom cosmology without big rip singularity. *Phys. Lett. B* **709**(4), 396–403 (2012)
83. S. Nojiri, S.D. Odintsov, Is the future universe singular: Dark Matter versus modified gravity? *Phys. Lett. B* **686**, 44–48 (2010)
84. P.M. Sá, Late-time evolution of the universe within a two-scalar-field cosmological model. *Phys. Rev. D* **103**, 123517 (2021)
85. W.L. Freedman et al., The Carnegie–Chicago Hubble Program. VIII. An independent determination of the Hubble constant based on the tip of the red giant branch. *Astrophys. J.* **882**, 34 (2019)
86. A.G. Riess, S. Casertano, W. Yuan, L.M. Macri, D. Scolnic, Large Magellanic Cloud Cepheid standards provide a 1% foundation for the determination of the Hubble constant and stronger evidence for physics beyond Λ CDM. *Astrophys. J.* **876**(1), 85 (2019)
87. G.C.F. Chen et al., A SHARP view of H0LiCOW: H_0 from three time-delay gravitational lens systems with adaptive optics imaging. *Mon. Not. R. Astron. Soc.* **490**(2), 1743–1773 (2019)
88. K.C. Wong et al., H0LiCOW-XIII. A 2.4 per cent measurement of H_0 from lensed quasars: 5.3σ tension between early- and late-Universe probes. *Mon. Not. R. Astron. Soc.* **498**(1), 1420–1439 (2020)
89. F.K. Anagnostopoulos, D. Benisty, S. Basilakos, E.I. Guendelman, Dark energy and dark matter unification from dynamical space time: observational constraints and cosmological implications. *JCAP* **06**, 003 (2019)
90. W. Yang, S. Pan, A. Paliathanasis, S. Ghosh, Y. Wu, Observational constraints of a new unified dark fluid and the H_0 tension. *Mon. Not. R. Astron. Soc.* **490**(2), 2071–2085 (2019)
91. D.L. Shafer, D. Huterer, Chasing the phantom: a closer look at Type Ia supernovae and the dark energy equation of state. *Phys. Rev. D* **89**(6), 063510 (2014)
92. A.G. Riess, L. Macri, S. Casertano et al., A 3 % solution: determination of the Hubble constant with the Hubble space telescope and wide field camera 3. *Astrophys. J.* **730**, 119 (2011)
93. A. Tripathi, A. Sangwan, H.K. Jassal, Dark energy equation of state parameter and its evolution at low redshift. *JCAP* **06**, 012 (2017)
94. S. Alam et al., The clustering of galaxies in the completed SDSS-III Baryon Oscillation Spectroscopic Survey: cosmological analysis of the DR12 galaxy sample. *Mon. Not. R. Astron. Soc.* **470**(3), 2617–2652 (2017)
95. S. Nesseris, L. Perivolaropoulos, Crossing the phantom divide: theoretical implications and observational status. *JCAP* **01**, 018 (2007)
96. J. Dutta, W. Khylllep, H. Zonunmawia, Cosmological dynamics of the general non-canonical scalar field models. *Eur. Phys. J. C* **79**(4), 359 (2019)
97. N. Tamanini, C.G. Böhrer, Generalized hybrid metric-Palatini gravity. *Phys. Rev. D* **87**, 084031 (2013)
98. P.M. Sá, Unified description of dark energy and dark matter within the generalized hybrid metric-Palatini theory of gravity. *Universe* **6**(6), 78 (2020)
99. T. Harko, F.S.N. Lobo, Beyond Einstein’s general relativity: hybrid metric-Palatini gravity and curvature-matter couplings. *Int. J. Mod. Phys. D* **29**, 2030008 (2020)
100. N. Das, S. Panda, Inflation and Reheating in $f(R, h)$ theory formulated in the Palatini formalism. *JCAP* **05**, 019 (2021)